

# BEAM DYNAMICS SIMULATIONS OF THE LANSCE LINAC

Frank Merrill and Lawrence Rybarcyk

LANSCE Division, Los Alamos National Laboratory, Los Alamos, New Mexico 87545 USA

## Abstract

Detailed beam dynamics calculations of the LANSCE Linac have been performed using multi-particle simulation codes. The LANSCE accelerator produces both  $H^+$  and  $H^-$  beams and is comprised of Cockcroft-Walton injectors, a 100 MeV drift-tube linac and an 800 MeV side-coupled linac. Several improvements to the simulations of  $H^+$  and  $H^-$  beams have recently been made. These include the use of more accurate input distributions and a better estimate of beam neutralization in the low-energy beam transport. Better estimates of the accelerating fields in the drift-tube linac have also been determined through measurements and modeling. With these improvements better agreement has been achieved between the predictions and measurements of RMS beam parameters and beam losses for both beams. The details of the simulations along with predictions are presented in comparison with measurements for both  $H^+$  and  $H^-$  beams.

## 1 INTRODUCTION

The LANSCE accelerator begins with two Cockcroft-Walton injectors that accelerate  $H^+$  and  $H^-$  beam to 750 keV. Each beam is transported in a separate low-energy beam transport (LEBT) to a common LEBT that transports both beams to the drift-tube linac (DTL). The DTL operates at 201.25 MHz and accelerates the beams from 0.75 to 100 MeV. The transition region (TR) consists of two beam lines, one for  $H^+$  and the second for  $H^-$ , and transports both beams from the DTL to the Side-Coupled Linac (SCL). The SCL operates at 805 MHz and accelerates the beams to 800 MeV.

Each LEBT contains quadrupole magnets set to transport and transversely match each beam into the DTL. A single-cell 201.25 MHz buncher in each upstream LEBT, referred to as the pre-buncher, and an identical buncher in the common LEBT, referred to as the main buncher, are used to prepare the longitudinal phase-space of the beams for DTL injection.

The DTL consists of four tanks, referred to as modules 1 through 4. Each DTL tank is driven by a separate rf power source. Quadrupole magnets inside the DTL drift-tubes are used to establish a singlet FODO lattice.

The two beam lines in the TR each contain four quadrupole magnets for transporting and transversely matching the beams into the SCL. The SCL is made of 44 modules, each fed by a separate rf power source. The SCL modules 5 through 12 accelerate beam from 100 to

211 MeV and consist of four bridge-coupled tanks each with 32-36 cells. Modules 13 through 48 accelerate from 211 to 800 MeV and consist of two bridge-coupled SCL tanks with 49-61 cells. Quadrupole doublets between tanks provide the focusing lattice required for transport of the beams through the SCL.

During typical LANSCE operation an average current of 1 mA of  $H^+$  is delivered to one experimental area while an average current of 76  $\mu A$  of  $H^-$  is transported to the Proton Storage Ring (PSR) for compression and subsequent delivery to a neutron spallation target. The 1 mA of  $H^+$  beam is presently achieved by accelerating a peak current of 16.5 mA at a pulse rate of 100 Hz and a pulse length of 625  $\mu s$ . The 76  $\mu A$  of  $H^-$  is delivered at 20 Hz and 575  $\mu s$  length with a 9.5 mA peak current. The  $H^-$  beam must also be "chopped" for injection into the PSR with a chopping duty factor of  $\sim 70\%$ .

## 2 SIMULATION TECHNIQUE

A modified version of PARMILA was used to model the beam transport through the LEBT, DTL and TR. The beam transport through the SCL was modeled using a modified version of CCLDYN, a PARMILA-like code used to model beam dynamics through coupled-cavity linacs. These simulation codes were used in previous studies[1] of the LANSCE linac and were modified to incorporate more of the details of the beam transports and accelerator.

Both the  $H^+$  and  $H^-$  simulations were performed using  $1 \times 10^5$  macro-particles to represent  $6.2 \times 10^8$   $H^+$  ions or  $3.7 \times 10^8$   $H^-$  ions at DTL injection. The two-dimensional mesh used by PARMILA and CCLDYN to calculate space-charge forces consisted of 800 mesh points, 20 radial points and 40 longitudinal points.

### 2.1 Input Distributions

The transverse phase-space input distributions were derived from measurements made at TDEM1, a slit-and-collector emittance station upstream of the DTL. To discriminate between signal and noise on the collector wires only those data bins above 2% of the peak were included in the generation of the input distribution. The measured distributions were then normalized and used as a discrete probability distribution for the Monte-Carlo creation of the horizontal and vertical input distributions.

The longitudinal phase-space input distributions were estimated with PARMILA by transporting mono-energetic, unbunched  $H^+$  and  $H^-$  beams through their

respective pre-bunchers and the common main buncher to the slit of TDEM1.

The transverse and longitudinal phase-space distributions were combined without correlations to produce the final input distributions. The resulting  $H^+$  and  $H^-$  input distributions at the entrance to the DTL are shown in Fig. 1 and 2, respectively.

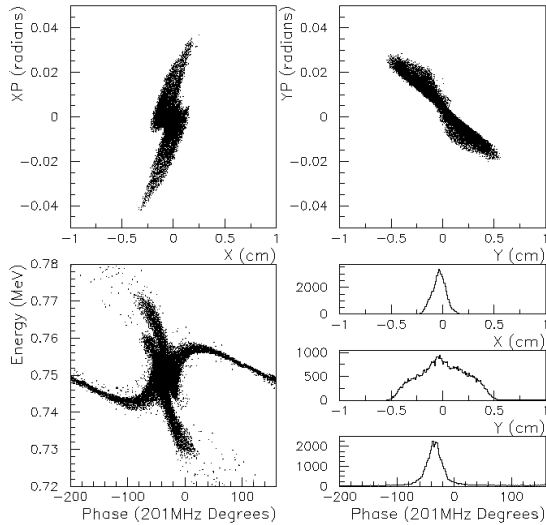


Figure 1: The simulated transverse and longitudinal  $H^+$  beam distributions at injection to the DTL.

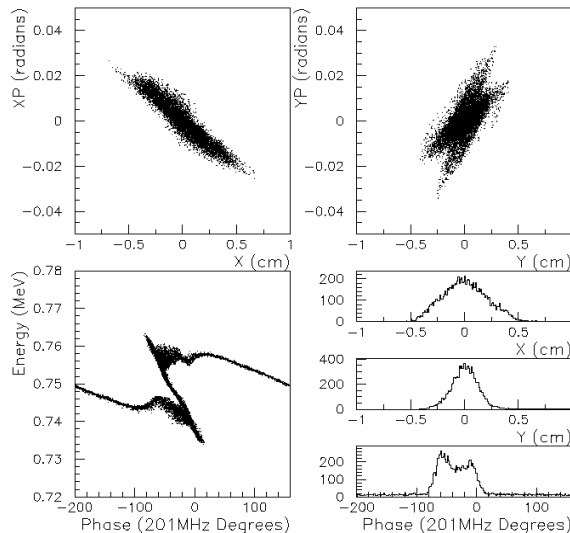


Figure 2: The simulated transverse and longitudinal  $H^-$  beam distributions at injection to the DTL.

## 2.2 Space-Charge Neutralization

The effects of space-charge neutralization in the common LEBT were estimated for both  $H^+$  and  $H^-$  beams from measurements made with TDEM1. For each beam the horizontal and vertical phase-space distributions at the slit position were measured along with the beam profiles at the collector position. The measured phase-space distributions were used as input in a PARMILA calculation to predict the beam profiles after a drift to the

collector location. An iterative search routine was used to determine the effective charge of the beam that resulted in the best agreement between the measured and predicted profiles. An effective peak of 85% of the measured  $H^+$  peak current and 75% of the measured  $H^-$  peak current were found to best reproduce the measured data.

The measured  $H^+$  and  $H^-$  currents were used in the DTL and SCL since the large magnetic and electric fields in these structures would quickly remove electrons or ions from the beam column. No neutralization effects were included in the simulations of the TR.

## 2.3 LEBT, DTL, TR and SCL Parameters

The field strengths of the quadrupoles in the LEBT, DTL, TR and SCL were determined from field-map data and present operating set points.

The phase and amplitude of the rf fields in the buncher and DTL cavities were determined through a combination of measurements and simulations. For these estimates a version of the PARMILA code was modified to include an option for simulating “phase scans”. This phase scan procedure uses an absorber-collector diagnostic to measure the transmitted beam current above an energy threshold versus the cavity rf phase. The phase centroid and width of the resultant distribution are related to the phase and amplitude of the rf fields in the cavity. For the bunchers, phase and amplitude settings were adjusted until measured phase scan results matched simulations that were based upon desired operating set points. For the DTL, phase scan simulations were performed for a range of amplitude and phase values that produced the desired output energy. Phase scan measurements were then performed with the DTL tanks at their production settings. Simulation results were interpolated to these measured phase scan parameters to extract an operating amplitude relative to the design amplitude for each tank. Simulations were then performed with these amplitudes and compared with measurements to obtain the operating phase set points of each of the DTL tanks.

The design phase and amplitude set points of the rf fields in each SCL module were used in the simulations.

## 3 SIMULATION RESULTS

The simulations were performed with beam started in the 750 keV LEBT and transported through the DTL and TR to the exit of the SCL at 800 MeV. Particle distributions were saved at various locations along the accelerator for analysis and comparison to measurements.

### 3.1 DTL Capture

The DTL capture ratio is the percent of the injected beam that is properly accelerated to 100 MeV through the exit of the DTL. This ratio is primarily determined by the longitudinal distribution at injection into the DTL and the settings of the DTL parameters. The two-buncher system

used at LANSCE results in a complicated longitudinal phase-space distribution at injection to the DTL. The simulated longitudinal  $H^+$  and  $H^-$  distributions at injection are shown in Fig. 1 and 2, respectively.

Simulations have shown that the structure of these distributions is primarily determined by the rf field strengths in the bunchers and the level of space-charge neutralization in the LEBTs. With the estimates of these parameters, described in section 2, the simulations accurately predict the capture for both  $H^+$  and  $H^-$  beams. The  $H^+$  capture was measured to be  $82\pm 1\%$  while simulations predict 80%. For the  $H^-$  beam a capture ratio of  $81\pm 1\%$  was measured while the simulations predict a ratio of 80%.

### 3.2 Beam Emittance

The measured transverse phase-space distributions at TDEM1 were used as input distributions for both  $H^+$  and  $H^-$  beam simulations. The next two emittance stations that were used for comparison with the simulations are located in the TR. Station one (TREM1) is located at the exit of the DTL and station two (TREM2) at the entrance to the SCL. The simulated and measured normalized RMS emittances at these locations are summarized in Table 1.

Table 1: Comparison of simulated and measured normalized RMS emittances for  $H^+$  and  $H^-$  beams in horizontal (H) and vertical (V) planes.

Emittance Station		$H^+$ RMS Emittance ( $\pi$ cm-mrad)		$H^-$ RMS Emittance ( $\pi$ cm-mrad)	
		Sim.	Meas.	Sim.	Meas.
TDEM1	H	$.93\times 10^{-2}$	$.93\times 10^{-2}$	$1.9\times 10^{-2}$	$1.9\times 10^{-2}$
	V	$.92\times 10^{-2}$	$.92\times 10^{-2}$	$2.5\times 10^{-2}$	$2.5\times 10^{-2}$
TREM1	H	$5.2\times 10^{-2}$	$3.1\times 10^{-2}$	$3.2\times 10^{-2}$	$2.8\times 10^{-2}$
	V	$2.7\times 10^{-2}$	$2.8\times 10^{-2}$	$5.1\times 10^{-2}$	$3.4\times 10^{-2}$
TREM2	H	$5.2\times 10^{-2}$	$3.7\times 10^{-2}$	$3.2\times 10^{-2}$	$2.9\times 10^{-2}$
	V	$2.7\times 10^{-2}$	$2.0\times 10^{-2}$	$5.0\times 10^{-2}$	$2.6\times 10^{-2}$

Although the simulated and measured RMS emittances agree, the higher order moments of the beam distributions in phase-space are different. The 95% emittance, which is the emittance value that includes 95% of the beam, includes information about these higher order moments. The predicted 95% emittance of the  $H^+$  beam in the TR is 2 times larger than the measured 95% emittance and the  $H^-$  95% emittance in the TR is 1.5 times larger than the measured value.

### 3.3 TR and SCL Losses

The simulations also predict the expected level of losses and the distribution of these losses along the SCL. Measurements of total losses have been made with current monitors that measure average current with an accuracy of  $\sim 1 \mu A$ . The loss distribution along the linac

has also been measured with loss monitors located along the SCL. A comparison between simulation and typical measured losses is shown in Table 2. The simulated and measured distribution of these losses is plotted in Fig. 3. Relatively good agreement has been achieved between simulation and measured losses, although the measured trend of increasing  $H^-$  losses along the linac has not yet been understood.

Table 2: Comparison of simulated and measured losses for  $H^+$  and  $H^-$  beams.

Between Modules	$H^+$ Losses		$H^-$ Losses	
	Sim.	Meas.	Sim.	Meas.
3-12	0.04%	0.1%	0.15%	< 1%
12-48	0.28%	< 0.1%	0.24%	< 1%

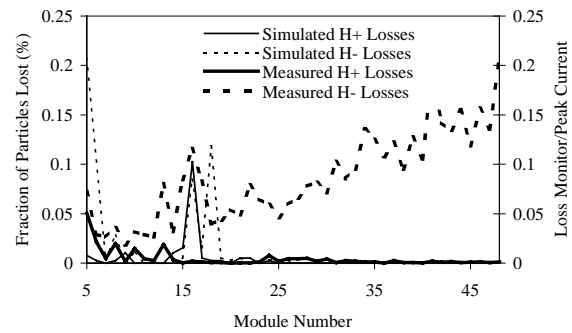


Figure 3: Fraction of particles lost versus module number from simulations (plotted against left axis) and measured losses scaled by peak current (plotted against right axis).

## 4 CONCLUSIONS

The recent improvements made to the beam dynamics simulations of the LANSCE linac have resulted in better agreement between simulation results and measurements. The most important of these were the use of input distributions derived from measurements, better estimates of space-charge neutralization effects in the LEBTs and the use of accurate estimates of the phase and amplitude of the DTL rf fields.

Because of the improved agreement between simulations and measurements this new model has been used to investigate upgrade scenarios with more confidence. The model is also presently being used to investigate possible sources of the smaller than predicted 95% emittance for both beams in the TR and possible effects that create the observed  $H^-$  losses along the SCL.

## 5 ACKNOWLEDGEMENTS

This work was supported by the U.S. Department of Energy.

## 6 REFERENCES

[1] R.W. Garnett et al. "Simulation Studies of the LAMPF Proton Linac", Proceedings of the Particle Accelerator Conference, Dallas Texas, May 1-5, 1995.